Ab Initio Studies of Vacancy-Defected Fullerenes and Single-Walled Carbon Nanotubes

LEI VINCENT LIU,[1] WEI QUAN TIAN,[2] YAN ALEXANDER WANG[1]

[1]*Department of Chemistry, University of British Columbia, Vancouver, British Columbia, Canada V6T 1Z1*

[2]*State Key Laboratory of Theoretical and Computational Chemistry, Institute of Theoretical Chemistry, Jilin University, Changchun, Jilin 130023, China*

Received 10 February 2009; accepted 8 April 2009
Published online 23 June 2009 in Wiley InterScience (www.interscience.wiley.com).
DOI 10.1002/qua.22298

ABSTRACT: The structures, stabilities, and electronic properties of the single-vacancy-defected fullerenes, C_{60} and C_{70}, and the single- and double-vacancy-defected single-walled carbon nanotubes (SWCNTs) were studied within density functional theory. The isomerization barriers for the single-vacancy-defected C_{60} on the triplet potential energy surface (PES) are lower than those on the singlet PES. The symmetric double-vacancy-defected (10,0) SWCNT is the most stable one among the models investigated. According to the analyses of frontier molecular orbitals (FMOs), nature bond orbitals, and local density of states, introduction of vacancy on the SWCNT decreases the band gap of semiconducting SWCNT, increases the band gap of conducting SWCNT, destructs the π conjugation of the FMOs, and gives rise to enhanced chemical activity. Int J Quantum Chem 109: 3441–3456, 2009

Key words: single-walled carbon nanotube; fullerene; vacancy defect

1. Introduction

Since the discoveries of fullerenes by Smalley and coworkers in 1985 [1] and carbon nanotubes by Iijima in the early 1990s [2], thousands of scientists all over the world have been attracted to the research field of fullerenes and carbon nanotubes. Such nanosystems have interesting properties and promising applications: for example, fullerenes as superconductors [3] and HIV protease inhibitors [4], and carbon nanotubes as chemical sensors [5], nanoscale electronics [6], hydrogen storage materials [7], etc. Recently, various methods of growing and engineering carbon nanotubes have become the driving forces to realize these applications [8].

Correspondence to: Y. A. Wang; e-mail: yawang@chem.ubc.ca
Contract grant sponsors: Natural Sciences and Engineering Research Council (NSERC) of Canada, and Jilin University.

Defects exist natively or can be introduced on carbon nanotubes and fullerenes. Defects on single-walled carbon nanotubes (SWCNTs) are classified into topological (containing rings other than hexagons), rehybridization (hybridization of the carbon atoms between sp^2 and sp^3), incomplete bonding defects (vacancies, dislocations, etc.), and doping with other elements (nitrogen, boron, etc.) [9]. Defects on fullerenes can also be categorized similarly. For example, the most common native defect on fullerenes, the Stone-Wales defect [10], formed by rotating the central bond of a pyracylene patch 90° on the surface, is a topological defect. Even number-vacancy-defected C_{60}, such as C_{58}, C_{56}, and C_{54}, can be made through laser irradiation [11]. Odd number-vacancy-defected C_{60}, such as C_{59}, C_{57}, C_{55}, and C_{53}, have been produced from the laser desorption ionization of $C_{60}O$ [12]. Such clusters have incomplete bonding defects.

Among all kinds of defects on fullerenes and SWCNTs, vacancy defects have very interesting properties and applications [13–35]. Vacancies on defected fullerenes were proposed to serve as the windows for atoms or small molecules to enter the cage in endohedral fullerene chemistry [13]. Vacancies on carbon nanotubes can be created by ion or electron irradiation [14, 15]. It has been shown that vacancy defects introduce localized electronic states on SWCNTs for chemical reactions [16] and can play the role of chemical connectors between two defected nanotubes [17] and the mediating role in the substitutional doping of nitrogen on the sidewall of a SWCNT [16, 18, 19].

Several theoretical studies have been devoted to investigate the properties of the vacancy-defected fullerene C_{60} [20–27]. The structures and stabilities of all the isomers of C_{59}, C_{58}, and C_{57} have been systematically studied with ab initio methods, but with some disagreements [24–27]. Earlier works [24, 25] reported that triplet C_{59}(5-8) is the more stable cluster of the two possible isomers of C_{59}: C_{59}(5-8) and C_{59}(4-9) [Figs. 1(b) and (c)]. The initial singlet C_{59}(4-9) isomer transforms into the singlet C_{59}(5-8) structure during a geometry optimization based on spin-unrestricted density functional theory (DFT) [25]. However, a recent work [26] found that singlet is the ground state for both C_{59}(5-8) and C_{59}(4-9) isomers. More interestingly, Andriotis et al. studied the single-vacancy-defected C_{60} in a C_{60} polymer by using tight-binding molecular dynamics and ab initio methods and found that two out of the three dangling bonds of the ideal single-vacancy defect do not recombine [27]. In this work, we have explored the isomerization pathways between these two isomers. For comparison, we also studied the single-vacancy-defected C_{70}, which is the second most abundant fullerene after C_{60}.

Vacancies on carbon nanotubes have also been studied recently [14–19, 28–35] for their effect on the conductance [28–30], the mechanical properties [32, 33], and the electronic properties [16, 19, 31] of carbon nanotubes. During the process of vacancy creation on carbon nanotubes, energetic electrons produce mostly single vacancies, whereas heavy ion irradiation produces mostly multivacancies [14]. Removing one or more carbon atoms from a carbon nanotube first produces ideal (but unstable) vacancies [see Figs. 2(a) and (d)]. Ajayan et al. have shown that carbon nanotube responds to the loss of the carbon atoms by surface reconstruction, resulting in vacancy-related point defects [15]. The nature of single vacancies and their related point defects has been studied systematically by Lu et al. with tight-binding method [35]. Double and triple vacancies and related defects have been studied by Mielke et al. [32] and Sammalkorpi et al. [33]. In these studies, however, the ground states of the defected nanotubes were not mentioned and the structural information has some contradictions. Lu and Pan reported that the symmetric 5-1DB (one pentagon and one dangling bond) defects [Fig. 2(c)] do not exist for the armchair-type SWCNT [35]. Even with the symmetric 5-1DB defect geometry as the starting structure, the asymmetric 5-1DB defect [Fig. 2(b)] was obtained [35]. However, the symmetric 5-1DB defect on the (5,5) SWCNT was shown to be stable by Mielke et al. [32]. To resolve such discrepancy, we have investigated the electronic properties of the single- and double-vacancy-defected SWCNTs (Figs. 2 and 3) with density functional methods.

2. Computational Details

Because of icosahedral (I_h) symmetry, all the carbon atoms are equivalent in C_{60}. While in C_{70}, there are five different types of symmetrically distinct carbon atoms, thus resulting in many possibilities for vacancy. For simplicity, we only considered the situation that the missing carbon atom is located in the pentagon at the pole of C_{70}. Geometry optimizations were performed with the hybrid DFT method, B3LYP [36, 37], with the standard 6-31G(d) basis set, and were followed by single-point calculations with B3LYP/6-311G(d). Natural bond or-

(a) Ideal single vacancy on C_{60} (b) C_{59}(4-9) (c) C_{59}(5-8)

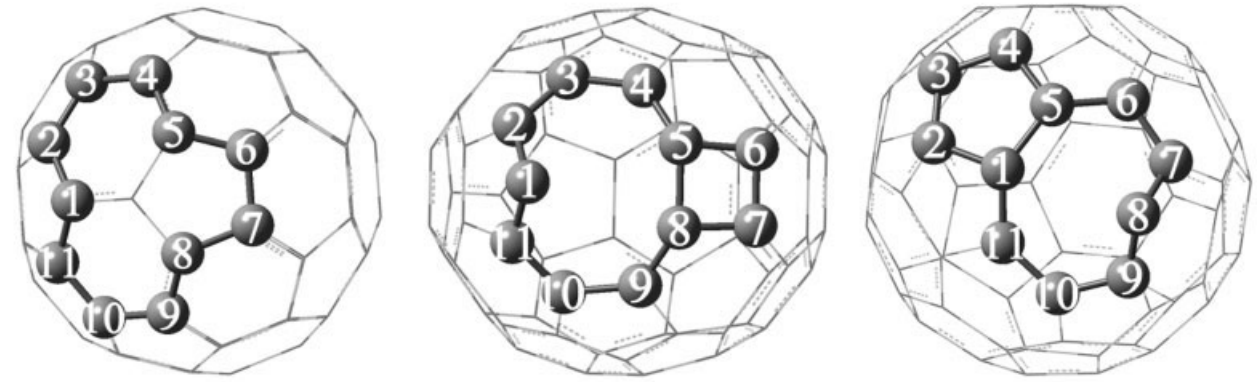

(d) Ideal single vacancy on C_{70} (e) C_{69}(4-9) (f) C_{69}(5-8)

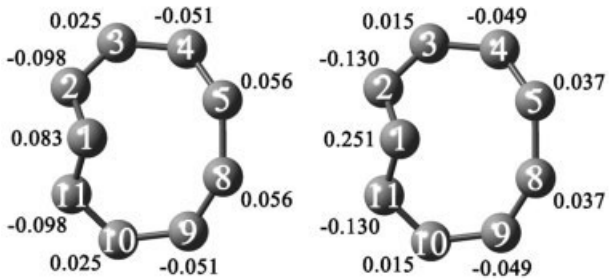

(g) Partial charges of the carbon atoms in the nonagon of the singlet (left) and triplet (right) C_{59}(4-9)

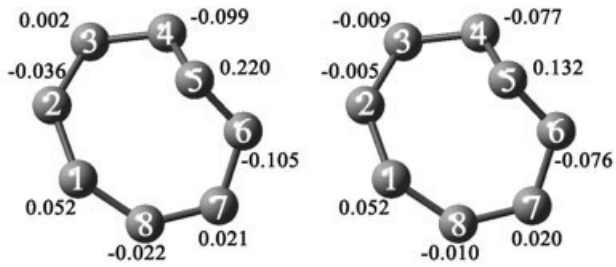

(h) Partial charges of the carbon atoms in the octagon of the singlet (left) and triplet (right) C_{59}(5-8)

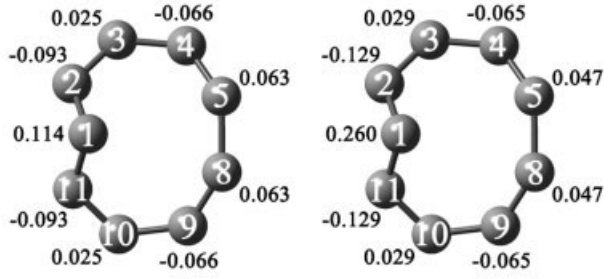

(i) Partial charges of the carbon atoms in the nonagon of the singlet (left) and triplet (right) C_{69}(4-9)

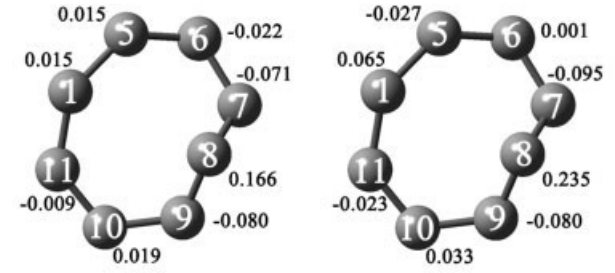

(j) Partial charges of the carbon atoms in the octagon of the singlet (left) and triplet (right) C_{69}(5-8)

FIGURE 1. Structures of the single-vacancy-defected C_{60} and C_{70} with partial charges of the important carbon atoms.

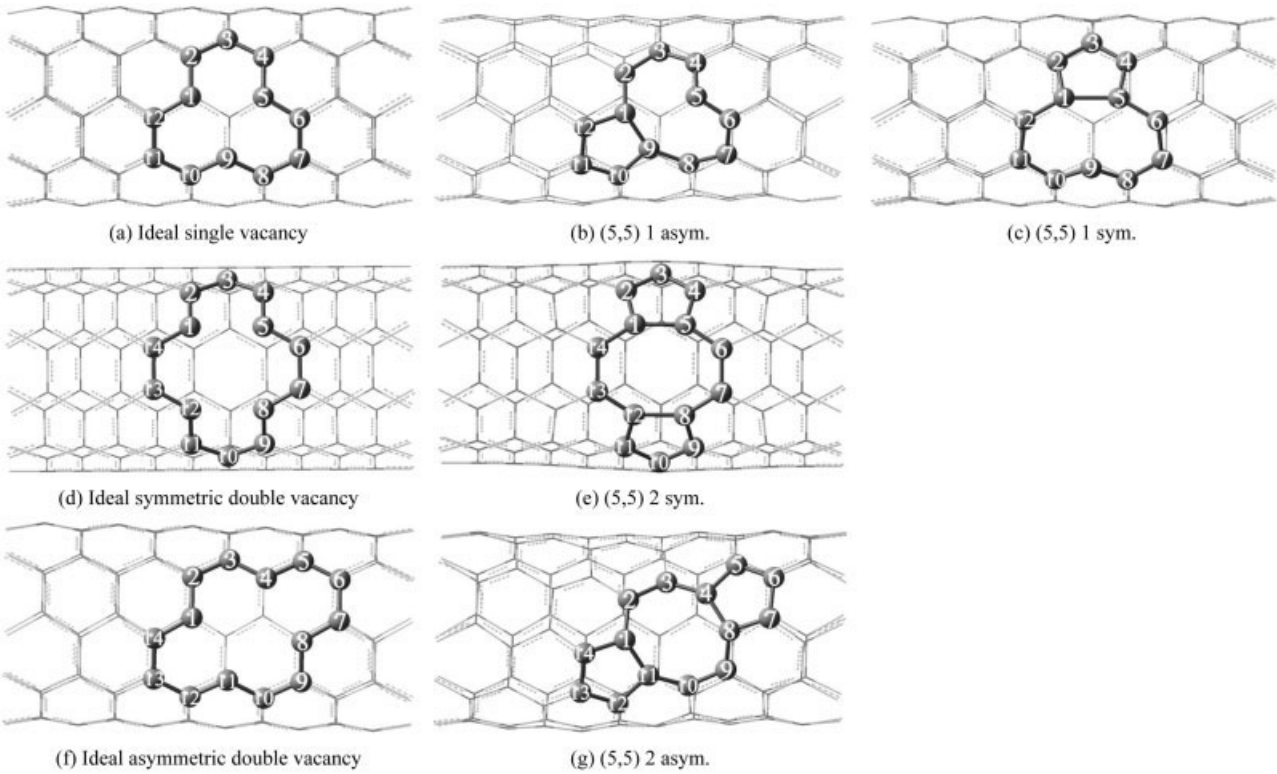

FIGURE 2. Structures of the ideal single and double vacancies and related defects on the (5,5) SWCNT.

bital (NBO) analysis [38] has been performed to determine the partial charge distribution and bonding characters of these systems. B3LYP/6-31G was employed to study the isomerization between C_{59}(5-8) and C_{59}(4-9) on the singlet and triplet potential energy surfaces (PESs).

The (5,5) and (10,0) SWCNTs were chosen to represent typical conducting armchair and semiconducting zigzag SWCNTs, respectively. Becke's (B) [39] exchange functional and Perdew's (PW91) [40] correlation functional based on the generalized gradient approximation combined with the 6-31G basis set were employed in geometry optimization and property prediction. With periodic boundary conditions (PBCs), the unit cells contain 100 and 120 carbon atoms for the (5,5) and (10,0) SWCNTs, respectively. The integrations of **k** space are achieved by using the default numbers of **k** points, 27 and 26 for the (5,5) and (10,0) SWCNTs, respectively.

Spin-restricted and spin-unrestricted calculations were carried out for the singlet and triplet electronic states, respectively. In light of previous numerical tests [41], the convergence criteria of all calculations were set very tight (e.g., 10^{-8} for the density convergence) so that the calculations are fully converged. All calculations were performed with the Gaussian 03 package [42].

3. Results and Discussion

3.1. VACANCY-DEFECTED FULLERENES

There are two types of bonds in C_{60}, the shorter double bonds and the longer single bonds, which were predicted to be 1.395 and 1.453 Å at the B3LYP/6-31G(d) level of theory, respectively, in good agreement with experiment (1.390 and 1.453 Å, respectively) [43]. The good performance of the B3LYP/6-31G(d) method in treating C_{60} gives us confidence in its application in the present study. The structures of C_{60} and C_{70} with ideal single vacancy and related point defects are shown in Figure 1, with important carbon atoms labeled numerically. In C_{59}, C1 forms a bond with C5 or C8 leading to the C_{59}(5-8) isomer (5 and 8 denoting the newly formed pentagon and octagon), or C5 forms a bond with C8 leading to the C_{59}(4-9) isomer (4 and 9 denoting the newly formed rectangle and nonagon). In C_{69}, C1 forms a bond with C5 or C8

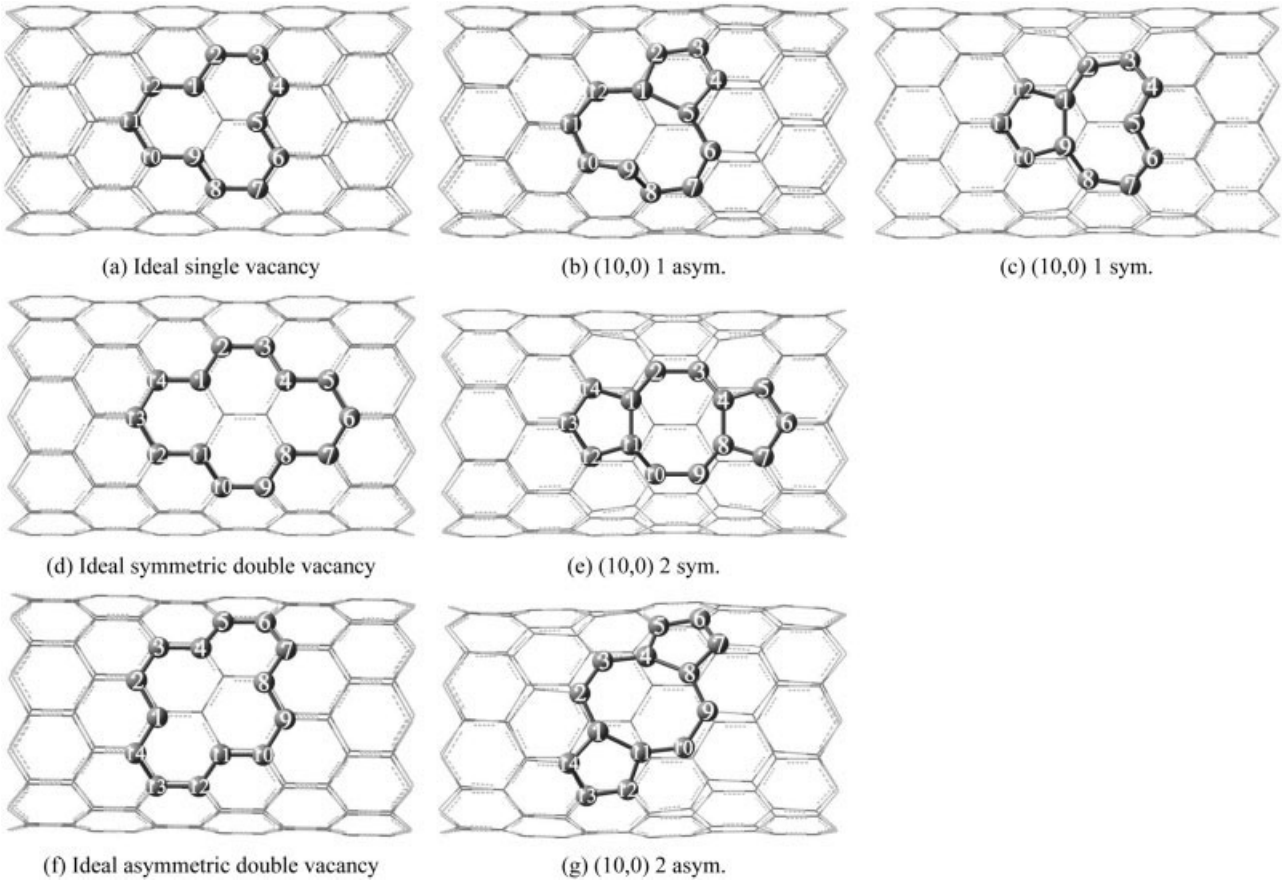

FIGURE 3. Structures of the ideal single and double vacancies and related defects on the (10,0) SWCNT.

leading to the C_{69}(5-8) isomer, or C5 forms a bond with C8 leading to the C_{69}(4-9) isomer. In each isomer, there is one unsaturated carbon atom in the nonagon for the (4-9)-type defects or in the octagon for the (5-8)-type defects.

Important bond lengths are tabulated in Table I. In comparison with the HF/3-21G and B3LYP/3-21G results [24] for the C_{59}(4-9) isomer, our B3LYP/6-31G(d) calculations predict shorter bond lengths for most bonds due to the larger basis set used. Table II lists the total and cohesive energies of the isomers predicted at the B3LYP/6-311G(d)//B3LYP/6-31G(d) level of theory. According to the cohesive energies, the single-vacancy-defected C_{70} is more stable than the single-vacancy-defected C_{60}. For the C_{59}(4-9) isomer, the singlet state is 0.82 kcal/mol more stable than the triplet state. For the C_{59}(5-8) isomer, the triplet state is 3.39 kcal/mol more stable than the singlet state. For the C_{69}(4-9) isomer, the singlet state is 2.32 kcal/mol lower in energy than the triplet state. For the C_{69}(5-8) isomer, the triplet state is 2.57 kcal/mol lower in energy than the singlet state. Thus, the triplet C_{59}(5-8) and C_{69}(5-8) isomers are the most stable isomers for C_{59} and C_{69}, respectively. However, one has to bear in mind that the small spin contamination in the spin-unrestricted calculations (see Table II) may artificially stabilize the triplet state over the closed-shell singlet state. Given such small energy differences, we can only conclude that the singlet and triplet electronic states of C_{59} and C_{69} have similar stabilities within the present DFT treatment.

For singlet C_{59}(4-9), the dangling carbon atom C1 forms single bonds with C2 and C11. The bond lengths of C1—C2 and C1—C11 are both 1.441 Å because of C_s symmetry. Based on the NBO analysis, there are two 2-center σ NBOs involving C1: σ(C1—C2) = 0.668 C1 ($sp^{2.33}$) + 0.745 C2 ($sp^{2.09}$) and σ(C1—C11) with the same bonding character. There are two lone-pair-type NBOs for C1: one is an $sp^{1.50}$ hybridized orbital with 1.79 electrons and the other one is a pure p orbital with 0.36 electrons. The

TABLE I

Bond lengths (in Å) of the single-vacancy-defected C_{60} and C_{70}, calculated at the B3LYP/6-31G(d) level of theory.

	C_{59}(4-9)		C_{59}(5-8)		C_{69}(4-9)		C_{69}(5-8)	
Bond	Singlet	Triplet	Singlet	Triplet	Singlet	Triplet	Singlet	Triplet
C1—C2	1.441	1.407	1.526	1.526	1.434	1.407	1.483	1.463
C1—C5							1.530	1.528
C1—C8			1.451	1.494				
C1—C11	1.441	1.407	1.495	1.421	1.434	1.407	1.446	1.488
C2—C3	1.389	1.398	1.462	1.477	1.382	1.391	1.370	1.372
C3—C4	1.479	1.479	1.448	1.458	1.469	1.470	1.448	1.452
C4—C5	1.396	1.401	1.420	1.399	1.397	1.403	1.410	1.419
C5—C6	1.453	1.454	1.378	1.357	1.454	1.453	1.457	1.472
C6—C7	1.431	1.428	1.435	1.466	1.430	1.426	1.442	1.452
C7—C8	1.453	1.454	1.426	1.411	1.454	1.453	1.418	1.397
C5—C8	1.599	1.608			1.582	1.591		
C8—C9	1.396	1.401	1.488	1.468	1.397	1.403	1.375	1.358
C9—C10	1.479	1.479	1.440	1.378	1.469	1.470	1.431	1.459
C10—C11	1.389	1.398	1.427	1.456	1.382	1.391	1.416	1.401

partial charges of the carbon atoms in the nonagon are shown in Figure 1(g) for the singlet and triplet C_{59}(4-9). C1 has +0.08 charge and its two neighbors have −0.10 charges in the singlet case, whereas in the triplet case, C1 has a much larger positive charge (+0.25) and its two neighbors also have larger negative charges (−0.13). The relevant frontier molecular orbitals (FMOs) of singlet C_{59}(4-9) are shown in Figures 4(a)–(d). Quite interestingly, there is nearly no electron population on C1 in the highest occupied molecular orbital (HOMO). The first orbital below the HOMO (HOMO–1) is mainly the lone-pair $sp^{1.50}$ hybridized orbital. The lowest unoccupied molecular orbital (LUMO) is mainly the lone-pair p unhybridized orbital. (Hereafter, we will use HOMO–n and LUMO+m to denote the nth molecular orbital below the HOMO and the mth molecular orbital above the LUMO, respectively.) The HOMO energy of singlet C_{59}(4-9) is −6.15 eV, higher than that of perfect C_{60} (−6.40 eV). The LUMO energy of singlet C_{59}(4-9) is −4.22 eV,

TABLE II

Energies of C_{60}, C_{59}(4-9), C_{59}(5-8), C_{70}, C_{69}(4-9), and C_{69}(5-8) at the B3LYP/6-311G(d)//B3LYP/6-31G(d) level of theory.

	E_{total} (Hartree)		E_{sa}[a] (kcal/mol)		ΔE[b] (kcal/mol)	
Model	Singlet	Triplet	Singlet	Triplet	Singlet	Triplet
C_{60}	−2286.5888		159.27			
C_{59}(4-9)	−2248.2431	−2248.2418 (2.05)[c]	156.76	156.75	2.51	2.52
C_{59}(5-8)	−2248.2690	−2248.2744 (2.05)	157.04	157.09	2.23	2.18
C_{70}	−2667.7857		160.16			
C_{69}(4-9)	−2629.4433	−2629.4396 (2.04)	158.05	158.02	2.11	2.14
C_{69}(5-8)	−2629.4629	−2629.4670 (2.05)	158.23	158.27	1.93	1.89

[a] The stability energy per atom, defined as E_{ts}/n, where E_{ts} is the energy difference between the isolated carbon atoms and the cluster and n is the total number of carbon atoms in the cluster.
[b] $\Delta E = E_{sa}$ (perfect fullerene) − E_{sa} (defected fullerene).
[c] The values in the parentheses are the $\langle S^2 \rangle$ values.

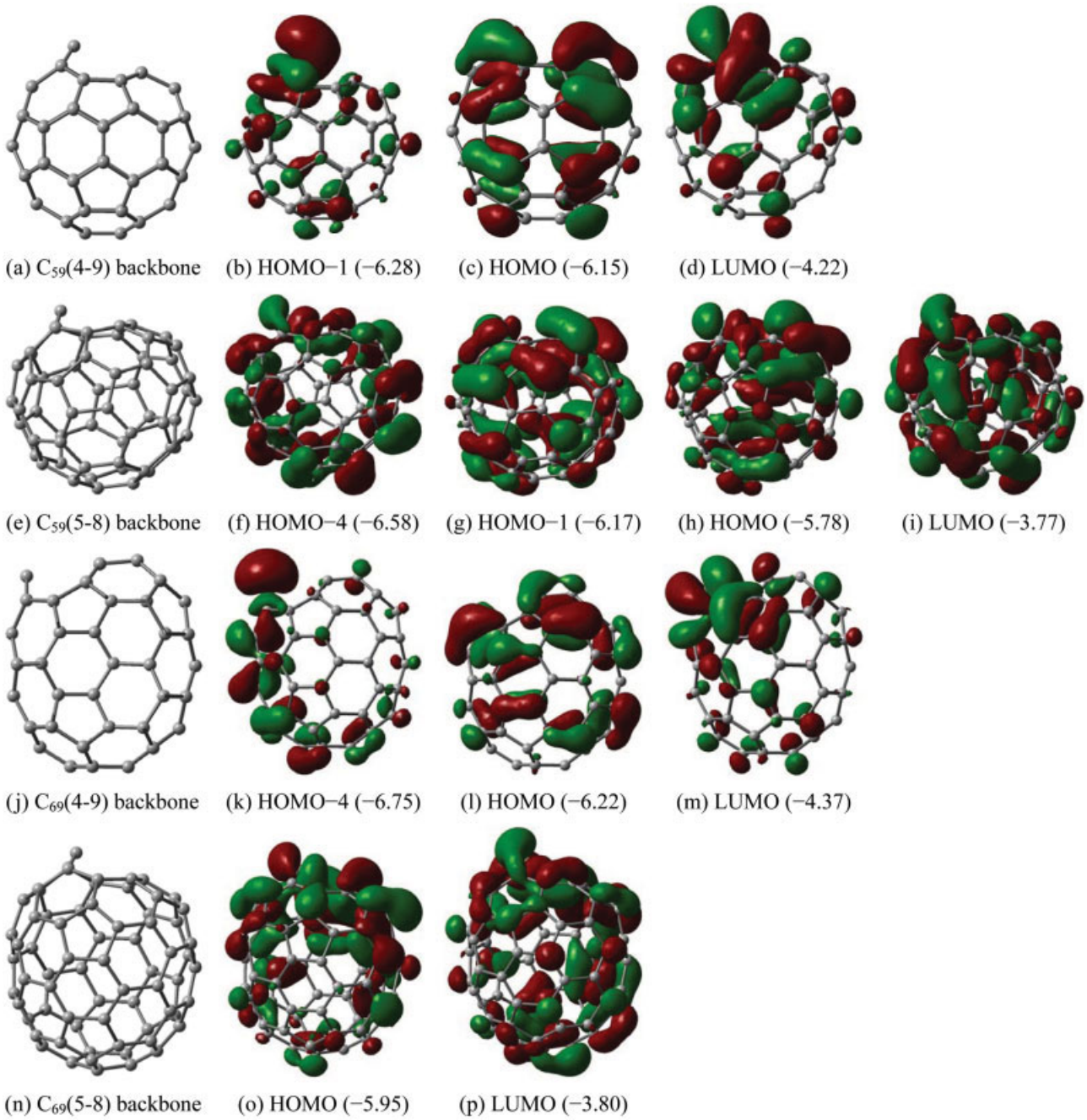

FIGURE 4. Frontier molecular orbitals of singlet C_{59}(4-9) (a–d), triplet C_{59}(5-8) (e–i), singlet C_{69}(4-9) (j–m), and triplet C_{69}(5-8) (n–p). HOMO–*u* (*x*) is the *u*th molecular orbital below the HOMO with orbital energy *x* eV. LUMO+*w* (*y*) is the *w*th molecular orbital above the LUMO with orbital energy *y* eV. [Color figure can be viewed in the online issue, which is available at www.interscience.wiley.com.]

lower than that of perfect C_{60} (−3.68 eV). Thus, the HOMO-LUMO gap is only 1.93 eV, smaller than that of perfect C_{60} (2.72 eV).

For triplet C_{59}(5-8), the dangling carbon atom C5 forms a single bond with C4 and a double bond with C6. The bond lengths of C5—C4 and C5═C6 are 1.399 and 1.357 Å, respectively. The point group of triplet C_{59}(5-8) is C_1. Based on the NBO analyses, there are three 2-center NBOs involving C5. Two NBOs represent the double bond of C5═C6:

σ(C5—C6) = 0.684 C5 ($sp^{1.51}$) + 0.729 C6 ($sp^{1.82}$) and π(C5—C6) = 0.720 C5 ($sp^{99.99}$) + 0.729 C6 ($sp^{99.99}$), and the other σ NBO represents the single bond of C5—C4: σ(C5—C4) = 0.685 C5 ($sp^{1.62}$) + 0.729 C4 ($sp^{2.17}$). There are also two lone-pair-type NBOs for C5: one is a $sp^{3.57}$ hybridized orbital with 0.947 electrons in α spin and the other one is an almost pure p orbital with 0.062 electrons in β spin. The α-spin FMOs are shown in Figures 4(e)–(i). The HOMO−4 and the HOMO contain the lone-pair p unhybridized orbitals [Figs. 4(f) and (h)]. The orbital energy of the α-spin HOMO of triplet C_{59}(5-8) is −5.78 eV, higher than that of perfect C_{60} (−6.40 eV). The orbital energy of the α-spin LUMO of triplet C_{59}(5-8) is −3.77 eV, slightly lower than that of perfect C_{60} (−3.68 eV). The orbital energy of the β-spin HOMO of triplet C_{59}(5-8) is −6.10 eV, higher than that of perfect C_{60} (−6.40 eV). The orbital energy of the β-spin LUMO of triplet C_{59}(5-8) is −4.41 eV, lower than that of perfect C_{60} (−3.68 eV). Thus, the α-spin HOMO-LUMO gap (2.01 eV) and the β-spin HOMO-LUMO gap (1.69 eV) are both smaller than that of perfect C_{60} (2.72 eV).

The electronic structures of singlet C_{69}(4-9) and triplet C_{69}(5-8), particularly around the vacancy defect (as shown in Figs. 1 and 4), are very similar to those of singlet C_{59}(4-9) and triplet C_{59}(5-8), respectively. Both HOMO-LUMO gaps are smaller than that of C_{70}.

A few years ago, Andriotis et al. studied the single-vacancy-defected C_{60} in a C_{60} polymer by using tight-binding molecular dynamics and ab initio methods [27]. In their study, two out of the three dangling bonds of the ideal single-vacancy defect do not recombine. About +0.5 charges were predicted to reside on the three carbon atoms with dangling bonds and the spin polarization occurs at the σ dangling bonds. In our study of the isolated single-vacancy-defected C_{60}, two out of the three dangling bonds do recombine. Only about +0.2 charge accumulates at the carbon atom with dangling bond and the two recombined carbon atoms. The spin polarization mainly localizes at the remaining carbon atom with dangling bond for both triplet C_{59}(5-8) and triplet C_{59}(4-9). The different conclusions might be caused by the different environments modeled by Andriotis et al. (in a C_{60} polymer) [27] and us (in gas phase). More refined theoretical treatment should be carried out to confirm the findings of Andriotis et al. [27].

More interestingly, these clusters with defect can be actually treated as carbenes. A carbene is a divalent carbon atom with four valence electrons, and its two nonbonding electrons can either lead to a singlet state or a triplet state. The simplest carbene is methylene. If methylene is linear, it will have two degenerate p orbitals, and each of the two nonbonding electrons will occupy one of these two p orbitals with the same spin, thus yielding a triplet ground state. If methylene is bent, the degeneracy of these two p orbitals is destroyed. The orbital perpendicular to the bent methylene is called "p," and the other orbital is called "σ" that hybrids with the s orbital and becomes stabilized. The more s character this σ orbital has, the bigger will be the energy gap between the σ and p orbitals. If the σ-p energy gap is big, the two nonbonding electrons will prefer to stay in the σ orbital with opposite spins, thus becoming a singlet carbene. If the σ-p energy gap is small, the two nonbonding electrons will prefer to stay in different orbitals with the same spin, thus producing a triplet carbene.

Our results indicate that the singlet carbene prefers to stay in the pentagon and the triplet carbene prefers to stay in the hexagon of the isomers of C_{59} and C_{69}. One reason for this scenario is that the triplet carbene prefers the bigger bond angle in the hexagon of the defect site, whereas the singlet carbene prefers the smaller bond angle in the pentagon of the defect site. Another reason is due to electronic effects. For example, according to NBO analyses, the σ orbitals of the carbenes of C_{59}(4-9) and C_{59}(5-8) are $sp^{1.50}$ and $sp^{3.57}$ hybridized, respectively. Thus, the σ-p energy gap of the carbene of C_{59}(4-9) is larger than that of C_{59}(5-8). On the other hand, the p orbital of the carbene of C_{59}(5-8) forms a π bond with one of its neighbor carbon atoms, while this is not the case for the carbene of C_{59}(4-9). This effect can lower the energy of the p orbital of the carbene of C_{59}(5-8), thus leading to a smaller σ-p energy gap, which also explains the larger stability of triplet C_{59}(5-8) and triplet C_{69}(5-8).

The isomerization pathways of C_{59}(4-9) and C_{59}(5-8) isomers on the singlet and triplet PESs were further explored. The relative energies, the structures of transition states, and the imaginary vibrational modes are shown in Figure 5. The energy of triplet C_{59}(5-8) is set as the reference zero-point. The barrier of singlet C_{59}(4-9) transforming into singlet C_{59}(5-8) is 35.69 kcal/mol and the reverse barrier is 54.50 kcal/mol. The barrier between singlet C_{59}(5-8)L (L denoting C1—C3 bond formation) and singlet C_{59}(5-8)R (R denoting C2—C3 bond formation) is 49.45 kcal/mol. The barrier of triplet C_{59}(4-9) transforming into triplet C_{59}(5-8) is 17.49 kcal/mol and the reverse barrier is 41.69 kcal/

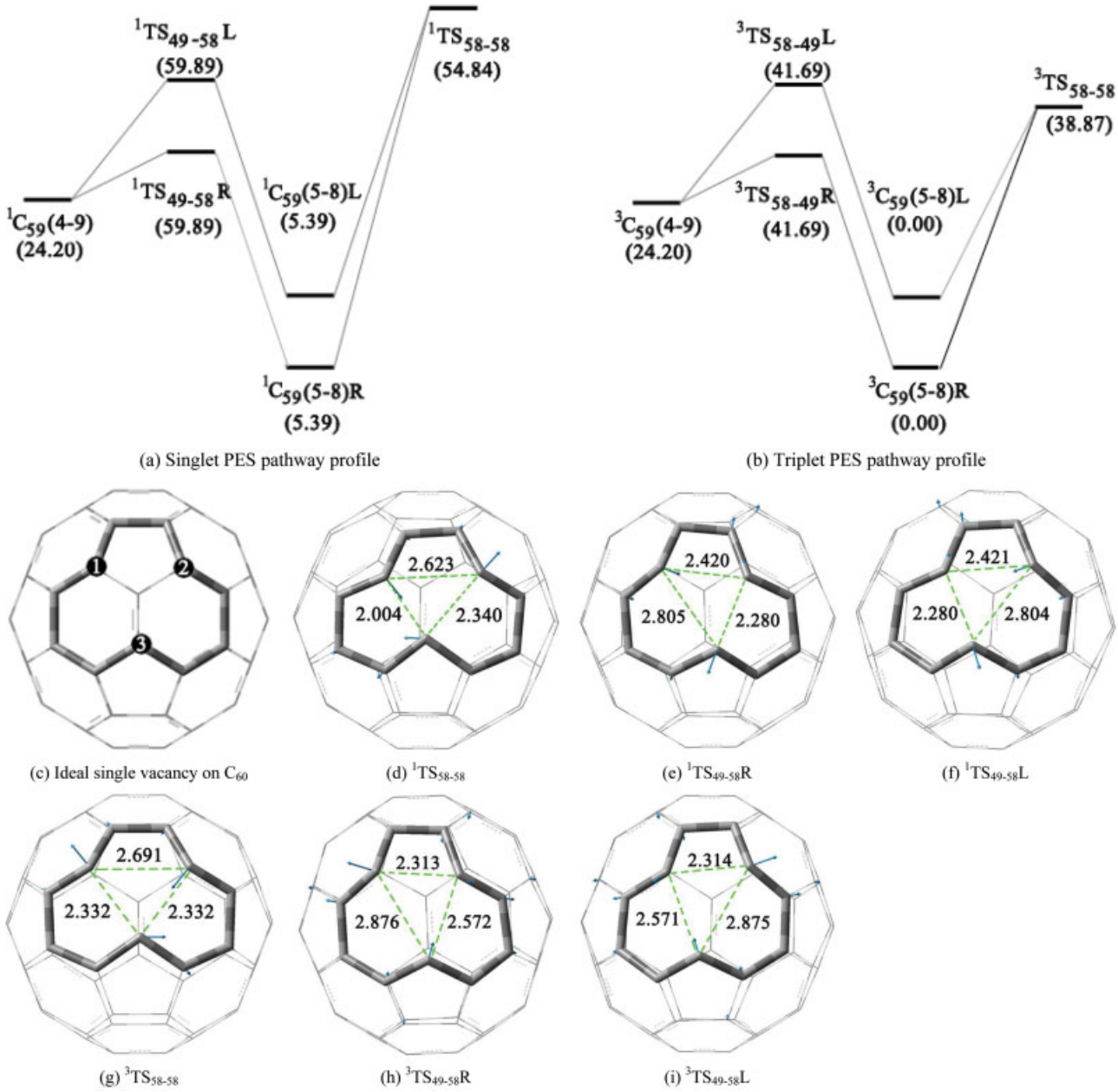

FIGURE 5. (a and b) Isomerization pathway profiles of the single-vacancy-defected C_{60} on the singlet and triplet potential energy surfaces, respectively (energies are in kcal/mol). (c) Ideal single vacancy on C_{60}; (d–i) Structures of the transition states (numbers are the atom distances in Å and the blue arrows represent the imaginary vibrational modes). In (f) and (i), L denotes the bond formation between C1 and C3, thus leading to a pentagon on the left. In (e) and (h), R denotes the bond formation between C2 and C3, thus leading to a pentagon on the right. [Color figure can be viewed in the online issue, which is available at www.interscience.wiley.com.]

mol. The barrier between triplet C_{59}(5-8)L and triplet C_{59}(5-8)R is 38.87 kcal/mol. Clearly, the isomerization takes place more feasibly on the triplet PES. Under the influence of strong external field or irradiation during the vacancy defect creation [11, 12, 14], such isomerization can occur easily. Both the relative energies of C_{59}(4-9) and C_{59}(5-8) and the isomerization barrier between C_{59}(4-9) and C_{59}(5-8) ensure that C_{59}(5-8) is the major product during the formation of C_{59}.

TABLE III

The vertical electron affinity (VEA), the adiabatic electron affinity (AEA), the vertical ionization potential (VIP), the adiabatic ionization potential (AIP) of C_{59}(4-9), C_{59}(5-8), C_{69}(4-9), and C_{69}(5-8).

Cluster	VEA	AEA	VIP	AIP
C_{59}(4-9)	3.42	3.32	7.36	7.29
C_{59}(5-8)	3.68	3.34	6.92	6.79
C_{69}(4-9)	3.66	3.55	7.35	7.30
C_{69}(5-8)	3.91	3.61	7.06	6.95

All energies are in eV.

Vertical and adiabatic values of the electron ionization and affinity energies (without the zero-point correction) for ground-state C_{59}(4-9), C_{59}(5-8), C_{69}(4-9), and C_{69}(5-8) are shown in Table III. The vertical electron affinity (VEA) or vertical detachment affinity is defined as the energy difference between the neutral cluster and its anion both at the equilibrium geometry of the anion [44]. The adiabatic electron affinity (AEA) or simple electron affinity is defined as the energy difference between the neutral cluster and its anion at their own equilibrium geometries [44]. The vertical ionization potential (VIP) is defined as the energy difference between the cation and its neutral cluster both at the equilibrium geometry of the neutral cluster. The adiabatic ionization potential (AIP) is defined as the energy difference between the cation and its neutral cluster at their own equilibrium geometries. The VEA and AEA of the C_{59}(4-9) and C_{69}(4-9) clusters are smaller than those of the C_{59}(5-8) and C_{69}(5-8) clusters, whereas the VIP and AIP of the C_{59}(4-9) and C_{69}(4-9) clusters are larger than those of the C_{59}(5-8) and C_{69}(5-8) clusters. The differences between the VEA and the AEA and between the VIP and the AIP for all these clusters are very small, indicating that the optimized geometries of the neutral clusters and their corresponding anionic and cationic clusters are close to one another.

3.2. VACANCY-DEFECTED SWCNTS

Perfect (5,5) and (10,0) SWCNTs were studied for comparison with defect SWCNTs. Removal of a single atom yields a 12-membered ring on both the (5,5) and (10,0) SWCNTs [Figs. 2(a) and 3(a)]. After surface reconstruction, a pentagon and a nonagon (contains an unsaturated carbon atom) appear in two different ways: one is asymmetric [Figs. 2(b) and 3(b)] and the other is symmetric [Figs. 2(c) and 3(c)] [33]. There are also two ways to lose two adjacent carbon atoms on both the (5,5) and (10,0) SWCNTs, resulting in 14-membered rings [Figs. 2(d) and (f), 3(d) and (f)]. After surface reconstruction, two pentagons and one octagon appear in symmetric [Figs. 2(e) and 3(e)] and asymmetric [Figs. 2(g) and 3(g)] patterns. No dangling bond is present for the double-vacancy defects. The energies and important bond lengths of these isomers are shown in Tables IV–VI.

The (5,5) SWCNT 1 asym. isomer [Fig. 2(b)] is more stable than the (5,5) SWCNT 1 sym. isomer [Fig. 2(c)]. The ground state of the (5,5) SWCNT 1 asym. isomer is singlet, whose energy is 2.26 kcal/mol lower than that of the triplet state. While the ground state of the (5,5) SWCNT 1 sym. isomer is triplet, whose energy is 9.66 kcal/mol lower than that of the singlet state. One should notice that the bridging bonds of the pentagon and the nonagon in the (5,5) SWCNT 1 sym. isomers are very weak: 1.846 and 1.871 Å in length for the singlet and triplet cases, respectively. However, for the asymmetric isomers, the bridges are typical C—C single bonds, with bond distances 1.579 and 1.565 Å for the singlet and triplet cases, respectively. The different defect structures of the (5,5) SWCNT 1 asym. and the (5,5) SWCNT 1 sym. isomers ensure the larger stability of the (5,5) SWCNT 1 asym. isomer. Our finding of the (5,5) SWCNT 1 sym. isomer agrees with the previous predictions [32] very well: the single-vacancy-defected (5,5) SWCNT does have the symmetric 5-1DB defect, which was not found by Lu et al. with tight-binding method [35].

For further definite confirmation, we carried out calculations on a finite model of the (5,5) SWCNT 1 sym. isomer, which has the same number of carbon atoms as in the PBC model and whose two open ends are capped by hydrogen atoms. In this finite model, the bridging bonds of the pentagon and the nonagon are 1.639 and 1.649 Å in length for the singlet and triplet cases, respectively, which are shorter than their counterparts in the PBC model. This is simply due to the relaxation of the constraint at the two open ends of the finite model. The energy of the triplet isomer is 14.10 kcal/mol lower than that of the singlet isomer, which agrees with the results of the PBC model. Thus, the existence of the symmetric 5-1DB defect on the single-vacancy-defected (5,5) SWCNT is without a doubt.

TABLE IV

Energies calculated at the BPW91/6-31G level of theory for the single- and double-vacancy-defected and perfect (5,5) and (10,0) SWCNTs.

System	E_{total} (Hartree)		E_{sa}[a] (kcal/mol)		ΔE[b] (kcal/mol)	
	Singlet	Triplet	Singlet	Triplet	Singlet	Triplet
(5,5) SWCNT	−3810.0481		169.20			
(5,5) SWCNT 1 asym.	−3771.7310	−3771.7274 (2.02)[c]	167.85	167.83	1.35	1.37
(5,5) SWCNT 1 sym.	−3771.6790	−3771.6944 (2.02)	167.52	167.62	1.68	1.58
(5,5) SWCNT 2 asym.	−3733.6917	−3733.6744 (2.02)	168.23	168.12	0.97	1.08
(5,5) SWCNT 2 sym.	−3733.5905	−3733.5735 (2.01)	167.58	167.48	1.62	1.72
(10,0) SWCNT	−4572.2690		170.31			
(10,0) SWCNT 1 asym.	−4533.9033	−4533.9102 (2.02)	168.94	168.98	1.37	1.33
(10,0) SWCNT 1 sym.	−4533.9535	−4533.9402 (2.02)	169.21	169.14	1.10	1.17
(10,0) SWCNT 2 asym.	−4495.8388	−4495.8144 (2.00)	169.13	169.00	1.18	1.31
(10,0) SWCNT 2 sym.	−4495.9168	−4495.9041 (2.00)	169.55	169.48	0.76	0.83

[a] The stability energy per atom, defined as E_{ts}/n, where E_{ts} is the energy difference between the isolated carbon atoms and the cluster and n is the total number of carbon atoms in the cluster.
[b] $\Delta E = E_{sa}$ (perfect SWCNT) $- E_{sa}$ (defected SWCNT).
[c] The values in the parentheses are the $\langle S^2 \rangle$ values.

The (5,5) SWCNT 2 asym. isomer [Fig. 2(g)] is more stable than its symmetric counterpart. For the (5,5) SWCNT 2 asym. isomer, the energy of the singlet state is 10.86 kcal/mol lower than that of the triplet state. The ground state of the (5,5) SWCNT 2 sym. isomers is also singlet, whose energy is 10.67 kcal/mol lower than that of the triplet state. The bond lengths of the bridging bonds of the (5,5)

TABLE V

Bond lengths (in Å) of the single- and double-vacancy-defected (5,5) SWCNTs.

Bond	(5,5) 1 asym.		(5,5) 1 sym.		(5,5) 2 asym.		(5,5) 2 sym.	
	Singlet	Triplet	Singlet	Triplet	Singlet	Triplet	Singlet	Triplet
C1—C2	1.463	1.466	1.435	1.431	1.426	1.436	1.442	1.441
C1—C5			1.846	1.871			1.687	1.664
C1—C9	1.579	1.565						
C1—C11			1.534	1.517				
C1—C12	1.475	1.462	1.541	1.528				
C1—C14					1.447	1.451	1.498	1.511
C2—C3	1.435	1.462	1.541	1.528				
C3—C4	1.430	1.442	1.421	1.422	1.451	1.457	1.414	1.414
C4—C5	1.402	1.394	1.435	1.431	1.435	1.444	1.442	1.441
C4—C8					1.534	1.517		
C5—C6	1.399	1.388	1.541	1.528	1.430	1.427	1.498	1.511
C6—C7	1.441	1.446	1.458	1.458	1.430	1.431	1.476	1.461
C7—C8	1.459	1.458	1.444	1.443	1.447	1.451	1.498	1.511
C8—C9	1.480	1.492	1.374	1.377	1.426	1.436	1.441	1.441
C8—C12					1.687	1.664		
C9—C10	1.439	1.448	1.374	1.377	1.464	1.456	1.414	1.414
C10—C11	1.424	1.421	1.444	1.443	1.451	1.457	1.414	1.414
C11—C12	1.427	1.427	1.458	1.458	1.435	1.444	1.442	1.441
C12—C13			1.430	1.427	1.498	1.511		
C13—C14			1.430	1.431	1.476	1.461		

TABLE VI

Bond lengths (in Å) of the single- and double-vacancy-defected (10,0) SWCNTs.

	(10,0) 1 asym.		(10,0) 1 sym.		(10,0) 2 asym.		(10,0) 2 sym.	
Bond	Singlet	Triplet	Singlet	Triplet	Singlet	Triplet	Singlet	Triplet
C1—C2	1.432	1.438	1.456	1.473	1.447	1.470	1.432	1.444
C1—C5	1.761	1.751						
C1—C9			1.560	1.530				
C1—C11					1.641	1.604	1.511	1.477
C1—C12	1.520	1.528	1.447	1.446				
C1—C14					1.456	1.457	1.429	1.440
C2—C3	1.419	1.416	1.437	1.437	1.483	1.469	1.452	1.435
C3—C4	1.421	1.421	1.432	1.439	1.478	1.494	1.432	1.444
C4—C5	1.460	1.452	1.404	1.393	1.434	1.445	1.429	1.440
C4—C8					1.640	1.604	1.512	1.477
C5—C6	1.485	1.493	1.404	1.393	1.413	1.408	1.431	1.428
C6—C7	1.452	1.458	1.432	1.439	1.422	1.425	1.431	1.428
C7—C8	1.423	1.422	1.437	1.437	1.456	1.457	1.429	1.440
C8—C9	1.400	1.385	1.456	1.473	1.447	1.471	1.432	1.444
C9—C10	1.384	1.372	1.447	1.446	1.483	1.469	1.453	1.435
C10—C11	1.444	1.448	1.424	1.423	1.478	1.494	1.432	1.444
C11—C12	1.470	1.472	1.424	1.423	1.434	1.445	1.429	1.440
C12—C13					1.413	1.408	1.431	1.428
C13—C14					1.422	1.424	1.431	1.428

SWCNT 2 sym. isomer are 1.687 Å, longer than those of the (5,5) SWCNT 2 asym. isomer (1.534 Å). The removal of one or two carbon atoms from the perfect (5,5) SWCNT decreases the cohesive energy per carbon atom by 1.35, 1.58, 0.97, and 1.62 kcal/mol for the (5,5) SWCNT 1 asym., 1 sym., 2 asym., and 2 sym. systems, respectively. Apparently, the (5,5) SWCNT 2 asym. isomer is the most stable one.

Direct band gaps of the perfect (5,5) SWCNT, singlet (5,5) SWCNT 1 asym. and 2 asym. isomers are 0.06, 0.11, and 0.30 eV, respectively. According to the density of states (DOS) plots [Figs. 6(a)–(c)], one can see that single- and double-vacancy defects introduce electronic states near the Fermi level. Introduction of vacancy defect in the perfect (5,5) SWCNT creates small band gap in the defected SWCNT and changes the DOS of the (5,5) SWCNT especially around the Fermi level. However, the essential electronic structure remains basically the same in the vacancy-defected (5,5) SWCNTs.

According to the DOS [Figs. 6(a) and (b)] and the FMO analysis [Figs. 7(a)–(c)] of the singlet (5,5) SWCNT 1 asym., we found that vacancy defects severely destruct the π conjugated system of the (5,5) SWCNTs and create localized electronic states around the nonagon. For the (5,5) SWCNT 2 asym. system [Figs. 7(d)–(f)], the HOMO and the LUMO are extended π bonds around the octagon and show weaker localization with respect to that of the (5,5) SWCNT 1 asym. system.

For the (10,0) SWCNT with vacancy defect, the (10,0) SWCNT 1 sym. isomer [Fig. 3(c)] is more stable than its asymmetric counterpart [Fig. 3(b)]. The ground state of the (10,0) SWCNT 1 sym. isomer is singlet, 8.34 kcal/mol lower in energy than the triplet state. The ground state of the (10,0) SWCNT 1 asym. isomer is triplet, 4.33 kcal/mol more stable than the singlet state. The bridging bonds of the symmetric isomers are 1.560 and 1.530 Å in length for the singlet and triplet states, respectively. However, the bridging bonds for the asymmetric isomers are much longer, with bond distances of 1.761 and 1.751 Å for the singlet and triplet states, respectively.

The (10,0) SWCNT 2 sym. isomer is more stable than its asymmetric counterpart. The energies of the symmetric and asymmetric isomers in their singlet states are 8.16 and 15.31 kcal/mol lower than their triplet states, respectively. The bridging bonds for symmetric and asymmetric isomers are around 1.511 and 1.620 Å in length, respectively. The removal of one or two carbon atoms from the perfect (10,0) SWCNT decreases the cohesive energy per carbon atom by 1.37, 1.10, 1.18, and 0.76 kcal/mol for the

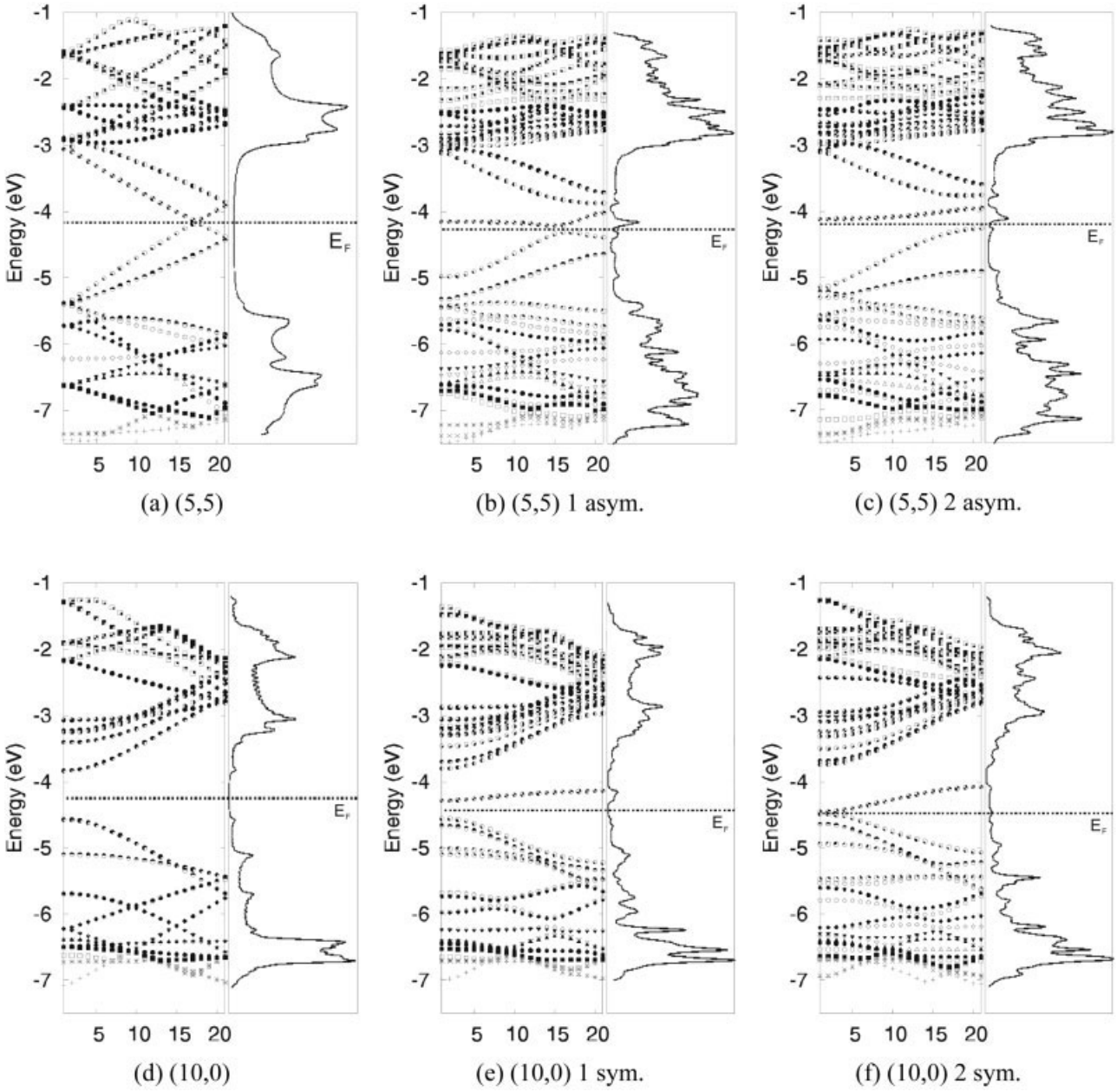

FIGURE 6. The change of the density of states after introducing vacancy defects on the (5,5) SWCNT (a–c) and the (10,0) SWCNT (d–f).

(10,0) SWCNT 1 asym., 1 sym., 2 asym., and 2 sym. isomers, respectively. Among them, the (10,0) SWCNT 2 sym. isomer is the most stable one. Band gaps of the perfect (10,0) SWCNT, singlet (10,0) SWCNT 1 sym. and 2 sym. isomers are 0.74, 0.27, and 0.03 eV, respectively. According to the DOS plots in Figures 6(d)–(f), we concluded that the single-vacancy defects introduce electronic states near the Fermi level and the double-vacancy defects bring electronic states across the Fermi level, enhancing the conductivity of the (10,0) SWCNT. Similar to the (5,5) SWCNT, the introduction of vacancy defects does not change the essential electronic structure of the (10,0) SWCNT according to the band structure and DOS. Also, vacancy defects destruct the π conjugated system of the (10,0) SWCNT as revealed by the FMOs shown in Figures 7(g)—(l). The LUMO of the (10,0) SWCNT 1 sym. system obviously has some

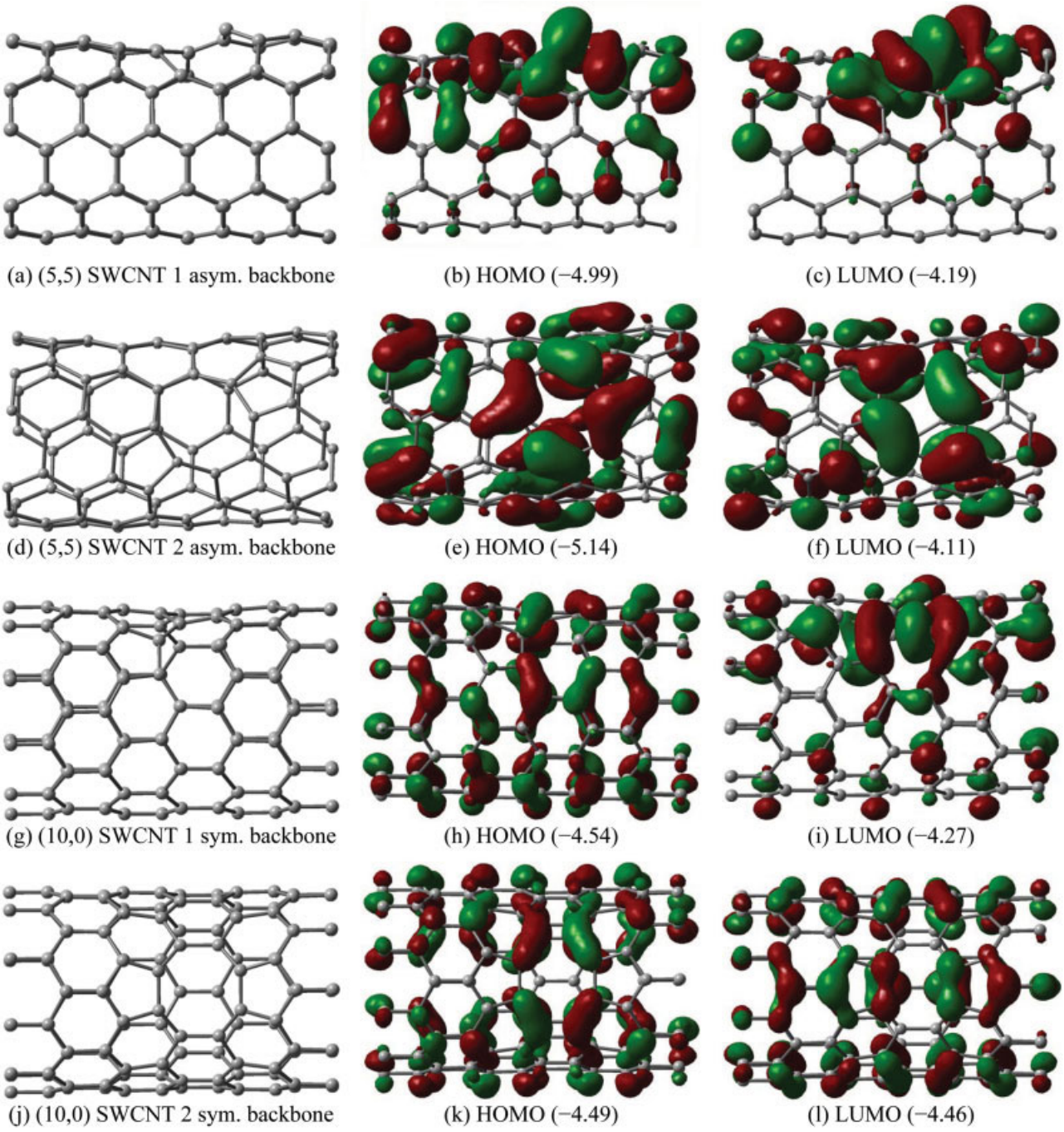

FIGURE 7. Frontier molecular orbitals of the (5,5) SWCNT 1 asym. cluster (a–c), the (5,5) SWCNT 2 asym. cluster (d–f), the (10,0) SWCNT 1 sym. cluster (g–i), and the (10,0) SWCNT 2 sym. cluster (j–l). HOMO (*p*) is the highest occupied molecular orbital with orbital energy *p* eV. LUMO (*q*) is the lowest unoccupied molecular orbital with orbital energy *q* eV. [Color figure can be viewed in the online issue, which is available at www.interscience.wiley.com.]

major contributions from the defect site. However, the localization of the electronic state is not as obvious as that on the (5,5) SWCNT near the Fermi level, possibly because of its larger band gap than that of the (5,5) SWCNT.

4. Conclusion

Within DFT, we have studied the structures, stabilities, and electronic properties of the single-va-

cancy-defected C_{60} and C_{70} and the single- and double-vacancy-defected SWCNTs in detail. We found that vacancy defects decrease the HOMO-LUMO gaps of C_{60} and C_{70}. The isomerization of the single-vacancy-defected C_{60} takes place more readily on the triplet PES than on the singlet PES. Among the isomers of the (5,5) SWCNT with vacancy defects, the singlet (5,5) SWCNT 2 asym. isomer is most stable. The symmetric single-vacancy-defected (5,5) SWCNT does exist, albeit not very stable. The symmetric singlet double-vacancy-defected (10,0) SWCNT is the most stable double-vacancy-defected SWCNT. Vacancy defects unavoidably destruct the π conjugation of the FMOs and thus enhance their chemical activity. On the other hand, vacancy defects on the SWCNTs might have completely opposite effects on the band gap of different SWCNTs: on the conducting (5,5) SWCNT, the band gap is increased, whereas on the semiconducting (10,0) SWCNT, the band gap is decreased.

ACKNOWLEDGMENTS

Most of the calculations were carried out on the Westgrid computational facility. L.V.L. gratefully acknowledges the Gladys Estella Laird and the Charles A. McDowell fellowships from the Department of Chemistry at the University of British Columbia. W.Q.T. thanks Prof. Yi-Song Zheng for constructive discussion.

References

1. Kroto, H. W.; Health, J. R.; O'Brien, S. C.; Curl, R. F.; Smalley, R. R. Nature 1985, 318, 162.
2. (a) Iijima, S. Nature 1991, 354, 56; (b) Iijima, S.; Ichihashi, T. Nature 1993, 363, 603.
3. Schmalz, T. G.; Seitz, W. A.; Klein, D. J.; Hite, G. E. J Am Chem Soc 1988, 110, 1113.
4. (a) Sijbesma, R.; Srdanov, G.; Wudl, F.; Castoro, J. A.; Wilkins, C.; Friedman, S. H.; DeCamp, D. L.; Kenyon, G. L. J Am Chem Soc 1993, 115, 6510; (b) Friedman, S. H.; DeCamp, D. L.; Sijbesma, R. P.; Srdanov, G.; Wudl, F.; Kenyon, G. L. J Am Chem Soc 1993, 115, 6506.
5. Kong, J.; Franklin, N. R.; Zhou, C. W.; Chapline, M. G.; Peng, S.; Cho, K. J.; Dai, H. J. Science 2000, 287, 622.
6. Avouris, P. Acc Chem Res 2002, 35, 1026.
7. Liu, C.; Fan, Y. Y.; Liu, M.; Cong, H. T.; Cheng, H. M.; Dresselhaus, M. S. Science 1999, 286, 1127.
8. (a) Hong, B. H.; Small, J. P.; Purewal, M. S.; Mullokandov, A.; Sfeir, M. Y.; Wang, F.; Lee, J. Y.; Heinz, T. F.; Brus, L. E.; Kim, P.; Kim, K. S. Proc Natl Acad Sci USA 2005, 102, 14155; (b) Hong, B. H.; Lee, J. Y.; Beetz, T.; Zhu, Y. M.; Kim, P.; Kim, K. S. J Am Chem Soc 2005, 127, 15336; (c) Wang, Y.; Kim, M. J.; Shan, H.; Kittrell, C.; Fan, H.; Ericson, L. M.; Hwang, W.-F.; Arepalli, S.; Hauge, R. H.; Smalley, R. E. Nano Lett 2005, 5, 997; (d) Cumings, J.; Collins, P. G.; Zettl, A. Nature 2000, 406, 586.
9. Charlier, J.-C. Acc Chem Res 2002, 35, 1063.
10. Stone, A. J.; Wales, D. J. Chem Phys Lett 1986, 128, 501.
11. O'Brien, S. C.; Heath, J. R.; Curl, R. F.; Smalley, R. E. J Chem Phys 1988, 88, 220.
12. Deng, J.-P.; Ju, D.-D.; Her, G.-R.; Mou, C.-Y.; Chen, C.-J.; Lin, Y.-Y.; Han, C.-C. J Phys Chem 1993, 97, 11575.
13. Saunders, M.; Jimenezazquez, H. A.; Cross, R. J.; Poreda, R. J. Science 1993, 259, 1428.
14. (a) Kiang, C.-H.; Goddard, W. A., III; Beyers, R.; Bethune, D. S. J Phys Chem 1996, 100, 3749; (b) Zhu, Y.; Yi, T.; Zheng, B.; Cao, L. Appl Surf Sci 1999, 137, 83; (c) Banhart, F. Rep Prog Phys 1999, 62, 1181.
15. Ajayan, P. M.; Ravikumar, V.; Charlier, J.-C. Phys Rev Lett 1998, 81, 1437.
16. Tian, W. Q.; Liu, L. V.; Wang, Y. A. In Handbook of Theoretical and Computational Nanotechnology; Rieth, M., Schommers, W., Eds.; American Scientific: Valencia, CA, 2006; Vol. 9, Chapter 10, p 499.
17. Terrones, M.; Terrones, H.; Banhart, F.; Charlier, J.-C.; Ajayan, P. M. Science 2000, 288, 1226.
18. Srivastava, D.; Menon, M.; Daraio, C.; Jin, S.; Sadanadan, B.; Rao, A. M. Phys Rev B 2004, 69, 153414.
19. Liu, L. V.; Tian, W. Q.; Wang, Y. A. J Phys Chem B 2006, 110, 1999.
20. Murry, R. L.; Strout, D. L.; Odom, G. K.; Scuseria, G. E. Nature 1993, 366, 655.
21. Sun, M.-L.; Slanina, Z.; Lee, S.-L. Fullerene Sci Technol 1995, 3, 627.
22. Turker, L. J Mol Struct (THEOCHEM) 2001, 571, 99.
23. Hu, Y. H.; Ruckenstein, E. J Chem Phys 2004, 120, 7971.
24. Hu, Y. H.; Ruckenstein, E. J Chem Phys 2003, 119, 10073.
25. Lee, S. U.; Han, Y.-K. J Chem Phys 2004, 121, 3941.
26. Ribas-Ariño, J.; Novoa, J. J. Phys Rev B 2006, 73, 035405.
27. Andriotis, A. N.; Menon, M.; Sheetz, R. M.; Chernozatonskii, L. Phys Rev Lett 2003, 90, 026801.
28. Igami, M.; Nakanishi, T.; Ando, T. J Phys Soc Jpn 1999, 68, 716.
29. Hansson, A.; Paulsson, M.; Stafstrom, S. Phys Rev B 2000, 62, 7639.
30. Igami, M.; Nakanishi, T.; Ando, T. Physica B 2000, 284–288, 1746.
31. Fagan, S. B.; da Silva, L. B.; Mota, R. Nano Lett 2003, 3, 289.
32. Mielke, S. L.; Troya, D.; Zhang, S.; Li, J. L.; Xiao, S. P.; Car, R.; Ruoff, R. S.; Schatz, G. C.; Belytschko, T. Chem Phys Lett 2004, 390, 413.
33. Sammalkorpi, M.; Krasheninnikov, A.; Kuronen, A.; Nordlund, K.; Kaski, K. Phys Rev B 2004, 70, 245416.
34. Rossato, J.; Baierle, R. J.; Fazzio, A.; Mota, R. Nano Lett 2005, 5, 197.
35. Lu, A. J.; Pan, B. C. Phys Rev Lett 2004, 92, 105504.
36. Becke, A. D. J Chem Phys 1993, 98, 5648.
37. Lee, C.; Yang, W.; Parr, R. G. Phys Rev B 1988, 37, 785.

38. (a) Glendening, E. D.; Carpenter, A. E.; Weinhold, F. NBO Version 3.1; University of Wisconsin: WI, 1995; (b) Reed, A. E.; Curtiss, L. A.; Weinhold, F. Chem Rev 1988, 88, 899.
39. Becke, A. D. Phys Rev A 1988, 38, 3098.
40. (a) Perdew, J. P.; Chevary, J. A.; Vosko, S. H.; Jackson, K. A.; Pederson, M. R.; Singh, D. J.; Fiolhais, C. Phys Rev B 1992, 46, 6671; (b) Perdew, J. P.; Burke, K.; Wang, Y. Phys Rev B 1996, 54, 16533.
41. Tian, W. Q.; Feng, J.-K.; Wang, Y. A.; Aoki, Y. J Chem Phys 2006, 125, 094105.
42. Frisch, M. J.; Trucks, G. W.; Schlegel, H. B.; Scuseria, G. E.; Robb, M. A.; Cheeseman, J. R.; Montgomery, J. A.; Vreven, T.; Kudin, K. N.; Burant, J. C.; Milliam, J. M.; Iyengar, S. S.; Tomasi, J.; Barone, V.; Mennucci, B.; Cossi, M.; Scalmani, G.; Rega, N.; Petersson, G. A.; Nakatsuji, H.; Hada, M.; Ehara, M.; Toyota, K.; Fukuda, R.; Hasegawa, J.; Ishida, M.; Nakajima, T.; Honda, Y.; Kitao, O.; Nakai, H.; Klene, M.; Li, X.; Knox, J. E.; Hratchian, H. P.; Cross, J. B.; Bakken, V.; Adamo, C.; Jaramillo, J.; Gomperts, R.; Stratmann, R. E.; Yazyev, O.; Austin, A. J.; Cammi, R.; Pomelli, C.; Ochterski, J. W.; Ayala, P. Y.; Morokuma, K.; Voth, G. A.; Salvador, P.; Dannenberg, J. J.; Zakrzewski, V. G.; Dapprich, S.; Daniels, A. D.; Strain, M. C.; Farkas, O.; Malick, D. K.; Rabuck, A. D.; Raghavachari, K.; Foresman, J. B.; Ortiz, J. V.; Cui, Q.; Baboul, A. G.; Clifford, S.; Coislowski, J.; Stefanov, B. B.; Liu, G.; Liashenko, A.; Piskorz, P.; Komaromi, I.; Martin, R. L.; Fox, D. J.; Keith, T.; Al-Laham, M. A.; Peng, C. Y.; Nanayakkara, A.; Challacombe, M.; Gill, P. M. W.; Johnson, B.; Chen, W.; Wong, M. W.; Gonzalez, C.; Pople, J. A. Gaussian 03, Revision B. 05; Gaussian, Inc.: Pittsburgh, PA, 2003.
43. Leclercq, F.; Damay, P.; Foukani, M.; Chieux, P.; Bellissent-Funel, M. C.; Rassat, A.; Fabre, C. Phys Rev B 1993, 48, 2748.
44. Rienstra-Kiracofe, J. C.; Tschumper, G. S.; Schaefer, H. F., III. Chem Rev 2002, 102, 231.